An Indoor Optical Wireless System Based on Different Spot Diffusing Geometries and A Diversity Receiver

Jamal M. Alattar and Jaafar M. H. Elmirghani

School of Engineering
University of Wales Swansea
Singleton Park, Swansea SA2 8PP, UK

Abstract: We evaluate the performance of a multi-beam transmitter system in an indoor environment where a diversity receiver is employed. The system's performance is evaluated under four new multi-line spot diffusing geometries and is compared with the performance of a single line of diffusing spots and with the conventional diffuse system (CDS). The performance is analysed under the influence of background noise produced by artificial ambient light sources and multipath propagation. A three-branch square-based pyramidal diversity receiver is used to optimise reception through a diversity selection scheme. An analysis as well as a comparison of the results obtained for signal delay spread and signal-to-noise ratio (SNR) is presented.

1. Introduction

Interest in optical wireless (OW) communication has increased in the past two decades in response to the increasing demand for bandwidth and in order to provide an alternative communication medium that overcomes the complexity of radio regulations. The use of infrared light to transmit data has advantages over radio frequency. In addition to making the communication bandwidth virtually unlimited thus avoiding license requirement, infrared also offers secure transmission against casual eavesdropping. Links operating in different rooms do not suffer infrared or radio interference.

Diffuse optical transmission systems do not rely on a line-of-sight path between the transceivers, thus enabling the system to operate in the existence of barriers. Signals reflect off walls and other surfaces and therefore undergo multiple paths before they reach the receiver's collection area. This will cause dispersion on the signal as the received pulse becomes spread therefore causing severe intersymbol interference (ISI) of the transmitted binary signals. Channel noise produced mostly by ambient light such as florescent and incandescent light sources introduce impairment into the received signal [1].

To mitigate these effects, a multi-spot narrow-beam transmitting technique has been proposed [2,3]. When used with a diversity receiver, the overall system performance improves [4,5]. The beams cast spots on the ceiling in a directional manner. These spots act as secondary Lambertian transmitters and improve the signal quality in the room [6]. The diversity receiver is able to select the best SNR branch since noise is directional in this environment. This work explores a number of spot diffusing geometries and compares their performance and the improvement offered in relation to a CDS.

2. System Setup

The conventional diffuse system (CDS) uses a single transmitter and a single wide field-of-view (FOV) receiver. Spot diffusing geometries can be realised with the use of a holographic optical diffuser [7,8]. A computer generated hologram is assumed to be mounted on the face of an infrared optical transmitting source employing an LED placed in the middle of an entirely empty room. The room has a moderate size of 4m × 8m × 3m (length × width × height). The ceiling and walls were modelled as Lambertian reflectors of the first order (n = 1). The reflectivity of the ceiling and the walls was set to 80%. On the communication plane CP (1m above the floor) where both the transmitter and receiver were placed and using infrared light, the transmitter produces multiple narrow beams that cast diffusing spots on the ceiling. A total optical transmission power of 1 W is evenly distributed among the number of spots produced in each case. The different configurations considered are:

i) a single line of 80 spots on the ceiling at x =2m and along the room width;

ii) three lines of 30 spots each on the ceiling at x = 1, 2 and 3m and along the room width

iii) two intersecting diagonals of 40 spots each on the ceiling

iv) a vertical line of 20 spots and a horizontal line of 60 spots intersecting in the centre of the ceiling

v) four lines of 20 spots each forming a diamond shape on the ceiling

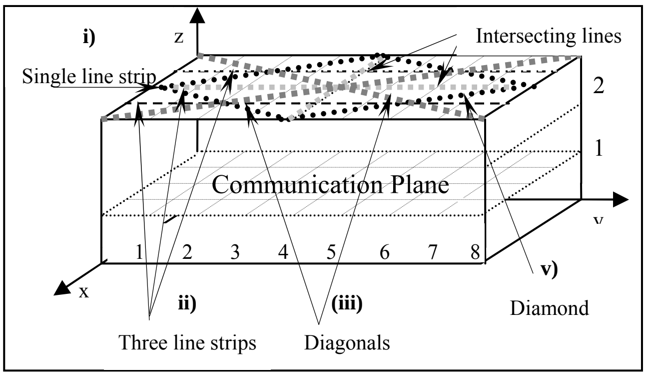

Figure 1: Spot diffusing geometries simulated

For all spot diffusing configurations, a diversity receiver was used. A three-branch square-based diversity optical receiver [4] with detectors of a 1 cm^2 (i.e., 1×10^{-4} m^2) active detection area on each branch was employed. The three branches have elevation angles of (35°, 90°, 145°) azimuth angles of (0°, 180°, 0°) and field of views of (40°, 70°, 40°).

A ray tracing simulation tool following, the algorithm presented by Barry et al [9], was designed for computing the impulse response of the channel under the various geometric configurations and for all receiver detectors.

Background noise from artificial and ambient light sources has been modelled as ideal Lambertian sources [10]. Eight halogen light sources (Philips PARA 80, which transmit the most stringent optical power) where placed equidistantly on the ceiling; 2m apart at Cartesian coordinates (1,1,3), (1,3,3), (1,5,3), (1,7,3), (3,1,3), (3,3,3), (3,5,3), (3,7,3). These spot lamps emit an optical power of 65W in a narrow beam with a propagation mode number n = 33.1 (corresponding to a hemisphere semi angle of 11.7^o). The optical noise power distribution was simulated for each receiver branch at receiver locations across two lines, x = 1m and x = 2m, with 1m spacing. Due to room symmetry, noise figures for receiver locations along the line x = 1m were identical to those at x = 3m. The total noise figure collected by a receiver branch detector at each receiver location was used in calculating the SNR from that branch. The receiver circuitry selects the output signal of the branch with the highest SNR value.

3. System Analysis

Ray tracing can be used to compute the power received in the room at any location due to a transmitter. The walls and ceiling are subdivided into small square-shaped reflecting elements where optical signals are known to reflect from such elements in a Lambertian fashion. Higher order reflections can be evaluated by considering each reflecting element as a secondary emitter. Reflections beyond second order are highly attenuated and are therefore not considered in this work.

The optical power received at a receiver's detector has a direct power component when there is an unobstructed line-of-sight (LOS) path between the transmitter and the receiver in addition to the power received from the first and second order reflections.

Hence,

$$P_r = P_d^{(0)} + \sum_{i=1}^{M} \left(dp_r^{(1)}\right)_i + \sum_{i=1}^{M} \left(dp_r^{(2)}\right)_i \qquad (1)$$

where M is the number of reflecting elements in the room.

With a receiver pointing upward with an elevation angle of 90^o in a down link channel (transmitter on ceiling facing down), the direct power P_d is given by

$$P_d^{(0)} = \frac{(n+1)}{2\pi \cdot R_d^2} \cdot P_S \cdot \cos(\theta_d)^{n+1} \qquad \textbf{(2)}$$

where R_d is the direct distance between the transmitter and receiver and θ_d is the angle between the normal to the receiver and the direct ray from the transmitter. The powers received due to reflections are given by

$$dp_r^{(1)} = \frac{(n+1)}{2\pi^2 \cdot R_1^2 \cdot R_2^2} \cdot P_S \cdot A_r \cdot \rho_1 \cdot \cos(\alpha)^n \cdot \cos(\beta) \cdot \cos(\gamma)^m \cdot \cos(\delta) \cdot rect(\delta / fov) \cdot dA_1 \qquad \textbf{(3)}$$

and

$$dp_r^{(2)} = \frac{(n+1)}{2\pi^3 \cdot R_1^2 \cdot R_3^2 \cdot R_4^2} \cdot P_S \cdot A_r \cdot \rho_1 \cdot \cos(\alpha)^n \cdot \cos(\beta) \cdot \cos(\alpha_1)^m \cdot \cos(\beta_1) \cdot dA_1 \cdot \rho_2 \cdot \cos(\gamma_1)^m \cdot \cos(\delta_1) \cdot rect(\delta_1 / fov) \cdot dA_2 \qquad \textbf{(4)}$$

where m is the reflection mode number of the reflective surfaces, A_r is the area of the detector, dA_1 and dA_2 are the areas of reflective elements of the first and second order reflections respectively, ρ_1 and ρ_2 are the reflection coefficients of surfaces 1 and 2. R_1 is the distance between the transmitter and reflective element of surface 1, R_2 is the distance between the reflective element of surface 1 and the receiver, R_3 is the distance between the reflective elements of surface 1 and surface 2 and R_4 is the distance between the reflective element of surface 2 and the receiver. The angles α, β, γ and δ correspond to the angle between R_1 and the normal to the transmitter, the angle between R_1 and the normal to reflective element of surface 1, the angle between R_2 and the normal to reflective element of surface 1 and the angle between R_2 and the normal to the receiver respectively. Likewise, α_1, β_1, γ_1 and δ_1 correspond to the angle between R_3 and the normal to the transmitter, the angle between R_3 and the normal to reflective element of surface 2, the angle between R_4 and the normal to reflective element of surface 2 and the angle between R_4 and the normal to the receiver respectively.

The function *rect(δ/fov)* is a step function which has a unity value when $\delta/fov \leq 1$ (i.e, the angle δ lies within the field of view of the receiver) and zero otherwise.

As the branches of an angle diversity receiver are elevated, therefore the angle of reception at the slanted face of the receiver has to be modified to

$$\cos(\delta) = \frac{\left|\overrightarrow{PR_x}\right|^2 + \left|\overrightarrow{ER_x}\right|^2 - \left|\overrightarrow{EP}\right|^2}{2 \cdot \left|\overrightarrow{PR_x}\right| \left|\overrightarrow{ER_x}\right|} \qquad \textbf{(5)}$$

where PR_x is the distance from the receiver to a point P located 1 meter on the detector's normal, ER_x is the distance from a reflective element to the receiver and *EP* is the distance from a reflective element to the point P.

The impulse response was calculated in time bins based on the time each ray takes to arrive at the detector. The time bin value was set to the time light takes to travel between neighbouring elements and is given by $\Delta t = \sqrt{\Delta A} / C$ where ΔA is the area of the differential element and C is the speed of light. This time bin smoothes the artificial discretisation process introduced (discrete reflecting elements).

The pulse response of the diffuse link is produced by convolving a pulse corresponding to the maximum optical power of the transmitter (1 Watt) and with duration equal to the inverse of the bit rate (50 Mbits/s in our case), with the time impulse of the system.

The transmitted signal undergoes temporal dispersion due to multipath reflections off the walls and ceiling causing the received pulse to spread along time. The delay spread of an impulse response is expressed as a root-mean-square function given by $D = \sqrt{\frac{\sum (t_i - \mu)^2 \cdot P_{r_i}^{\ 2}}{\sum P_{r_i}^{\ 2}}}$ where t_i is the delay time of the received optical power P_{r_i} (P_{r_i} reflects the impulse response $h(t)$ behaviour) and μ is the mean delay given by $\mu = \frac{\sum t_i \cdot P_{r_i}^{\ 2}}{\sum P_{r_i}^{\ 2}}$.

As the positions of the transmitter and receiver and the reflecting elements are fixed, therefore the delay spread is considered as deterministic for given transmitter and receiver locations.

The SNR associated with the received signal can be given by

$$SNR = \left(\frac{R \times (P_{s1} - P_{s0})}{\sqrt{\sigma_{pr}^{\ 2} + \sigma_{bn}^{\ 2}} + \sqrt{\sigma_{pr}^{\ 2} + \sigma_{bn}^{\ 2}}} \right)^2 \quad \textbf{(6)}$$

where R is the detector responsivity (R = 0.5 A/W in this study), P_{s1} and P_{s0} are the received power associated with a signal one and zero respectively and σ_{pr}^2 and σ_{bn}^2 are the receiver and background noise variances respectively. The PIN-BJT receiver structure [11] was assumed with bandwidth of 70 MHZ and σ_{pr} = 2.7 pA/√Hz.

4. Results

The performance of the various geometries was evaluated in terms of SNR and delay spread. The results are shown in Figure 2 along the x = 1m line which represents the worst performance line in the room in general. The x = 2m line in most cases falls underneath the transmitter (room centre) and the performance is better. Variations are possible but are not studied here. The x = 3m line is similar to the x = 1m line due to symmetry in the room and the diffusing spots geometries considered.

Results were evaluated for the CDS in order to establish a reference. The CDS in Figure 2 a) employs a wide field-of-view receiver facing upwards. As a result, this system is severely affected by background noise due to spot lights on the x = 1m line (worst performance line in the room). The SNR is seen to oscillate at a period given by the spacing of the spot lights on the ceiling. Furthermore, the presence of the CDS transmitter in the room centre results in an envelope (CDS SNR crests) that peaks at the room centre. Figure 2 b) shows the delay spread for the various geometries. The CDS has minimum delay spread at the room centre; i.e., close to the transmitter. Nearer the walls (y = 1m and y = 7m) the delay spread increases due to reflections from the walls and the increased distance to the transmitter.

The single line strip system has a uniform high SNR along the room as its diversity receiver avoids line-of-sight links with the spot lights that produce the noise. The delay spread for this system is also uniform as shown in Figure 2 b) and is due to the distributed spots which enhance the signal in a more symmetric fashion throughout the room. The three line strips produce a performance worse than that of the line strip. The overall transmitted power is the same in both cases. This can be understood by observing that a spot diffusing system with a very large number of spots approaches a conventional diffuse system where the whole ceiling acts as a reflector.

The intersecting diagonal spot lights are less symmetric in that a large number of spots cluster at the room centre. This produces a high SNR at the room centre as shown in Figure 2 a) that decays towards the room edges. The associated delay spread for this geometry (Figure 2 b) is predictably low at the room centre as the receiver is equidistant from all spots (delay variation is small) and is far from the reflecting walls. The delay spread increases toward y = 1m and y = 7m. The perpendicularly intersecting lines of spots has a similar trend to the diagonal spot geometry, but performs better due to the larger clustering of spots at room centre and the better distribution of spots (coverage follows the rectangular nature of the room). The diamond geometry produces poor performance. The centre of the room has no spot coverage, therefore the SNR is low at the room centre and improves slightly towards the room edges. The delay spread oscillates along the x = 1m line as the receiver moves from room centre (low delay spread, equidistant to spots) to room edges. As the line of spots is intersected the delay spread drops but increases near the walls due to reflections.

The line strip geometry produced the best performance and the results show that the spot distribution is important as a balance has to be struck between coverage and total population of ceiling with spots which reverts to CDS. Transmitter mobility warrants further consideration.

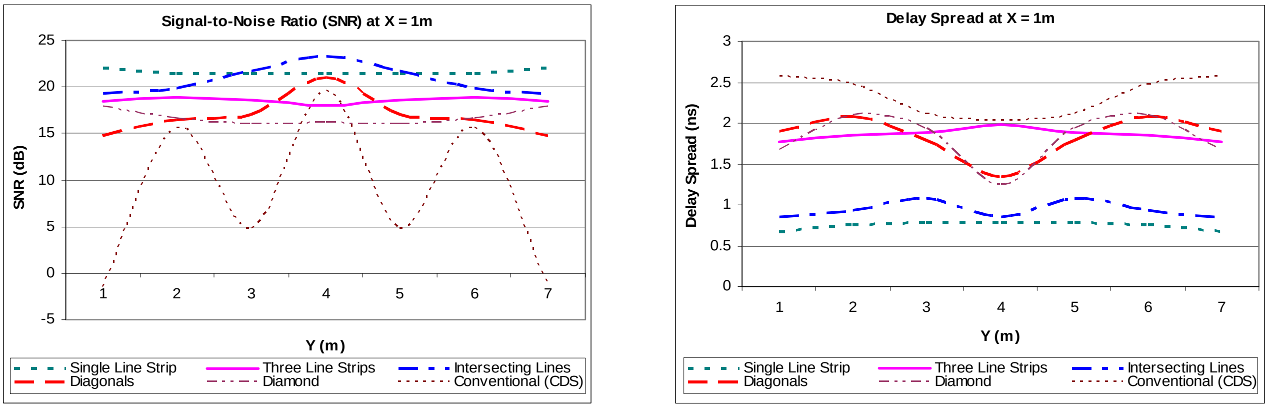

a) Signal-to-Noise Ratio (SNR) b) Delay Spread

Figure 2: systems performance with receiver at x = 1m and along the room width

5. Conclusions

In this paper, we investigated the performance of an indoor optical wireless channel with four other geometries of spot diffusing and have compared the results to the known CDS case. The results show that the intersecting lines configuration achieves significant SNR improvement in the centre of the room over the single line of spots. Lower delay spread values were obtained when the receiver is placed mid way between a wall and the centre of the room with the diamond configuration. The results also show that a careful balance has to be established between room coverage using spots and the total population of the ceiling with spots which causes the spot diffusing system to revert to a CDS case. Future work will consider the impact of transmitter mobility on these systems.

6. References

[1] A. J. C. Moreira, R. T. Valadas, and A. M. de Oliveira Duarte, “Optical interference produced by artificial light,” Wireless Networks, vol. 3, pp. 131-140, 1997.

[2] S. T. Jivokova and M. Kavehard: “Multispot diffusing configuration for wireless infrared access,” IEEE Trans. Commun., vol. 48, pp. 970-978, June 2000.

[3] A. G. Al-Ghamdi and J. M. H., Elmirghani, “Line Strip-Diffusing Transmitter Configuration for Optical Wireless Systems Influenced by Background Noise and Multipath Dispersion,” IEEE Trans. Commun., vol. 52, no. 1, pp. 37-45, Jan. 2004.

[4] A. G. Al-Ghamdi and J. M. H., Elmirghani, “Spot diffusing technique and angle diversity performance for high speed indoor diffuse infra-red wireless transmission,” IEE Proc.-Optoelectron., Vol. 151, No. 1, pp. 46-52, February 2004.

[5] G. Yun and M. Kavehrad, “Spot diffusing and fly-eye receivers for indoor infrared wireless communications,” in Proc. 1992 IEEE Conf. Selected Topics in Wireless Communications, Vancouver, BC, Canada, June 25–26, pp. 286–292, 1992.

[6] J. R. Barry, J. M. Kahn, E. A. Lee, and D. G. Messerschmitt, “High-speed nondirective optical communication for wireless networks,” IEEE Network Mag., vol. 5, pp. 44-54, Nov. 1991.

[7] M. R. Pakravan, E. Simova, and M. Kavehard, “Holographic diffusers for indoor infrared communication systems,” Int. J. Wireless Inform. Networks, vol. 4, no. 4, pp. 259-274, 1997.

[8] P. L. Eardley, D. R. Wiely, D. Wood, and P. McKee, “Holograms for optical wireless LANS,” Inst Elect. Eng. Proc. Optoelectron., vol. 143, no. 6, pp. 365-369, Dec. 1996.

[9] John R. Barry, et al. “Simulation of Multipath Impulse Response for Indoor Wireless Optical Channels,” IEEE Journal on selected areas in communication, Vol. 11, no. 3, pp. 367–379, April 1993.

[10] Hsun-Hung Chan, et. al, “Performance of Optical Wireless OOK and PPM System Under the Constraint of Ambient Noise and Multipath Dispersion”, IEEE Communications Magazine, pp. 83-87, Dec. 1998.

[11] J. M. H. Elmirghani, H. H. Chan, and R. A. Cryan, “Sensitivity evaluation of optical wireless PPM systems utilising PIN-BJT receivers,” Inst. Elect. Eng. Proc. Optoelectron., vol. 143, no. 6, pp. 355-359, Dec. 196.